TECHNICAL MEMORANDUMS

NATIONAL ADVISORY COMMITTEE FOR AERONAUTICS

No. 800

THE DESIGN OF FLOATS

By W. Sottorf

Luftfahrtforschung
Vol. 14, Nos. 4-5, April 20, 1937
Verlag von R. Oldenbourg, München und Berlin

14, Nos. 4-5, April 20, 1937, pp. 137-167.

G, gross weight of airplane, (kg).

P, impact load, (kg).

E, unloading, (kg).

γ, specific weight, (kg/m^3).

$M_{h\ st}$, moment about the transverse axis through the point of the step, (mkg).

v, speed, (m/s).

v_{max}, speed at maximum resistance, (m/s).

v_{start}, get-away speed, (m/s).

$\epsilon = \frac{W}{A}$, planing number.

$c_a' = \frac{A}{\gamma\ b_{st}^3}$, load coefficient.

$c_{mh} = \frac{M_{h\ st}}{\gamma\ b_{st}^4}$, moment coefficient.

$F = \frac{v}{\sqrt{g\ b_{st}}}$, Froude number.

λ, scale of model.

α = trim, angle with the horizontal of the tangent to the keel at the step.

α_{opt}, trim of minimum resistance. (Best trim.)

σ_1, angle of wing chord to the tangent to the keel at the step.

ζ, included angle of dead rise (dihedral angle).

I. THE FORMS OF DOMESTIC AND FOREIGN FLOAT SYSTEMS

A survey of the types of seaplane developed here and abroad within the last years, discloses the views of the designers as regards suitable designs and dimensions of float systems are still greatly at variance.

Figure 1 shows that the beam at the step b_{st} versus gross weight G for flying boats and against G/2 for twin-float seaplanes in logarithmic scale. The load coefficients $c_a' = \frac{G}{\gamma\, b_{st}^3}$, are used as the parameters and, according to Newton's general law of similitude, are constant for similarly loaded float systems. Establishing with $c_a' = 2.92$ constant a lower, and with $c_a' = 0.364$ constant an upper, limit on the cluster of points, the respective limiting beams of float systems that have been built are $b_{st} = 0.7 \left(\frac{G}{\gamma}\right)^{1/3}$ and $1.4 \left(\frac{G}{\gamma}\right)^{1/3}$, and for equal load, are in the ratio of 1:2.

Figure 2 shows, to the same scale, midship sections and sheer plans for a selection of well-known types which, by applying this law of similarity, have been reduced to the common gross weight of 1 ton for both hulls and float. It illustrates how differently beam, length-beam ratio, length of forebody, total length, or position of step and cross section were selected by the various designers, and it is not to be assumed that these designs are of equal value. The differences in form are in part conditioned by different requirements of the float system. So if any standardization of the form of the float system is to be attempted, the requirements must first be defined.

II. REQUIREMENTS OF A FLOAT SYSTEM

a) The water resistance must be small and the angle of attack of the planing bottom to be reached by pulling up must at the instant of get-away, be great enough to be able to bring the angle of attack of the wing into the range of $c_{a_{max}}$.

The greater the excess thrust and the lower the get-away speed, the smaller the take-off time and take-off run.

b) The spray formed should be small.

c) The impact forces excited during take-off and landing should be small. They increase with the seaway, for which reason the strength specifications are grouped according to stresses in order to be able to modify the requirements regarding seaworthiness.

d) During take-off the airplane must have no tendency to oscillate about the transverse axis which may become the cause of delay of take-off and of porpoising at higher speed.

e) Riding at anchor, the airplane should be weatherly, so that bow will head into the wind; it further should be stable about all horizontal axes in a side wind, whose velocity is in proportion to the required seaworthiness. In twin-float seaplanes the minimum stability occurs when down by the stern, and therefore is determined by the form of the float. In flying boats and seaplanes with a central float, it occurs under transverse inclination, in which case the size and distance of the side floats are decisive.

f) While maneuvering the airplane must respond quickly to air and water rudders.

g) The air resistance must be small.

The effect of the form parameters on points a) to c) will be discussed after the take-off process has been described. Data for a qualitative opinion regarding point d) are altogether lacking at the present time. The characteristics cited under points e) and f) are largely dependent on the airplane design as a whole and therefore will not be discussed further in the present paper.

III. TAKE-OFF WITH SPECIAL REFERENCE TO THE EFFECT OF THE AFTERBODY

Figure 3 shows a take-off diagram with the usual curves of the forces and trims. It may be divided into four speed stages, in which the flow forms differ markedly and consequently, the effect of the afterbody on the take-off is markedly different.

First stage: At the beginning of the take-off there is no difference hydrodynamically, between planing and displacement craft, since flow is taking place over the limiting edges of the planing bottom at the sides and on the step and the sides themselves are wetted. The form of the hull, in itself unfavorable, produces a relatively high resistance, whose effect on the get-away, however, remains small as this stage is quickly passed through, because of the great excess of thrust. At around $\frac{1}{2} v_{max}$ (the speed of maximum resistance) the relative speed of the water at the step is already so great that break-away takes place. But the trough or wake formed aft of the step is as yet short and the major part of the afterbody is still in contact with the water. Considering the water forces on the forebody and afterbody separately (fig. 4), the afterbody carries almost half the load. Because of the negative angle of the afterbody keel, the resultant normal force acting on the afterbody surfaces has a horizontal component opposite to the resistance of the forebody and lowers the total resistance. The resultant of the total water forces has moved forward but little from its position at rest, so that the trim of the float remains small.

Second stage: As the impact pressure increases, the length of the furrow aft of the step increases and the contact between the bottom of the afterbody and the water travels correspondingly further aft. The process of getting on step is characterized by a sudden emersion of the float occurring within a narrow speed range and accompanied by marked increase in trim.

The maximum resistance of the float lies a little higher - usually between 0.3 and 0.4 v_{start}. Only the after part of the afterbody is then in contact with the water; the sides are completely free. The afterbody, with

its share of the lift, tends to decrease the resistance, even at the hump. The resultant water force has reached its most forward position in the range of maximum resistance, with which moment and trim also reach their maximum values. The trim is reduced more or less by the noseheavy moment of the afterbody in the proportion that the afterbody shares in the lift.

The effect of the afterbody in stages I and II is such that the curve of the resistance of a forebody towed without afterbody is the envelope of the curves of combinations between forebody and afterbody. The more favorable the support by the afterbody, the lower the hump, which is shifted toward higher speeds on account of it (and not as a result of the later formation of the planing condition).

Third stage: The furrow aft of the step has become so long that the conflux in the plane of symmetry of the waves coming from the sides of the planing bottom and bounding the furrow, lies behind the float so that the roach formed there no longer strikes the afterbody. In this stage of pure planing, the float at normal trim touches the water only with a portion of the planing bottom lying forward of the step. As the impact pressure increases, the pressure area becomes shorter and then, since the wings unload the airplane more effectively, the resultant water force shifts backward and the trim of the float decreases. Toward the end of this stage the natural trim of the float has continuously decreased to a very small angle. By increased pulling up, the float is held at a medium trim, favorable in relation to the total resistance.

Fourth stage: In the stage before the get-away, contact of the afterbody with the water spray is unavoidable. In a float with dead rise, the beam of the bottom becomes greater than the natural beam of the bottom area under pressure because of the small load remaining, as a result of which a heavy spray escapes backward (fig. 5) over the open outer edges of the bottom. To insure a short takeoff the airplane must be pulled up to get-away (α_{max} = angle of afterbody keel), which increases the effect of the spray on the afterbody. The tangential contact of this water with the afterbody increases the frictional resistance so much that under certain circumstances the total resistance equals the propeller thrust despite the small load left on the water and get-away becomes impossible.

The control of the projected spray takes place in the part of the bottom near the chines. Systematic tests have shown that the water is kept flat when the section is turned to the horizontal, according to figure 11b, with not too small a radius of curvature. With a straight section (fig. 11a) the water rises high in continuation of the direction of the bottom, while with pronounced recurvature at the chine (fig. 11c) it is directed against the surface where it is reflected at a high angle. Figure 12 shows the spray patterns of a model in which the left half of the sections were curved downward according to figure 11c, while those of the right half terminated in the horizontal (fig. 11b). The differences in the form of the spray are readily seen. A recurvature at the chine that goes beyond the horizontal, has a very unfavorable effect on landing shock (reference 4) and is therefore to be avoided.

Longitudinal steps of every kind have proved unsuitable in systematic tests of planing surfaces and models with respect to resistance; neither do they offer any advantages relative to impact forces.

Depth and Location of Step; Angle of Afterbody

The location of a straight afterbody relative to the furrow formed aft of the step is determined by the depth of step and the angle between forebody and afterbody.

It has been established that contact of the stern with the solid water behind the furrow at maximum resistance has a favorable effect, while contact of the stern with the spray in the stage before get-away has an adverse effect.

At maximum resistance, therefore, small depth of step and small angle between forebody and afterbody are advantageous, while just before get-away great depth of step and large angle of afterbody keel (forebody alone: optimum) are advantageous as seen in figure 13, which presents the results of model tests with different depths of step and angles of afterbody. The results from the forebody are appended as limiting values.

	Depth of step	Angle of afterbody keel
Model 0.3 VH a	0	7°
" 0.3 VH b	0.017 b_{st}	7°
" 0.3 VH c	0.05 b_{st}	7°
" 0.3 VH d	0.10 b_{st}	7°
" 0.3 VH e	0.05 b_{st}	9.5°
" 0.3 V		

The expected decrease in resistance from the float with greater depth of step (limit value: forebody alone) to the float with zero depth of step appears in the stage before the maximum.

At maximum resistance the conditions on the stepped float are as yet the same. But for step depth 0, it appears that the air space in course of formation behind the break is filled up again from the rear, so that the getting-on-step is greatly retarded and the maximum resistance, as a result, increases further. Even if by further increase of speed, the planing condition has been reached the resistances are from two to three times as high as for the stepped floats.

In the stage before get-away the float with the greatest depth of step (or the forebody alone) shows the lowest resistance, while the float with zero depth of step is altogether unusable.

A depth of step of from 0.04 to 0.05 b_{st} has proved satisfactory. On high-speed airplanes, it is reduced to 0.025 b_{st} in order to reduce the air resistance.

The maximum resistance becomes greater with large angles of afterbody keel, while the spray effect falls shortly before get-away and through it, the rise of resistance occurring there, is reduced.

Because of the dependence of the form of wake on dead rise, load, and speed, no generally valid statement can be made regarding the optimum angle between afterbody and forebody; 7° has proved to be a good average value.

Naturally, the arguments refer to the ratio:

$\frac{\text{forebody length } l_V}{\text{over-all length } l_L}$, defining the location of the step.

With decreasing l_V/l_L, the favorable effect of the afterbody increases in stages I and II, while in stage IV, a large l_V/l_L is desired, in order to reduce the area of the afterbody hit by the spray. $l_V/l_L = 0.55$ is a good value for floats. For flying boats having aft of the second step a tail extension with larger angle of keel, the length of the afterbody (measured to the second step) may be shortened to about $\frac{l_V}{l_L} = 0.65$ to favor the forebody, if stage IV needs a reduction in resistance, inasmuch as the tail extension insures ample stability by the stern. l_V/l_L is the only parameter which, under certain conditions, causes a differentiation between float and flying-boat hull.

V. THE DVL STANDARD FLOAT

The DVL standard float - a float design evolved on the foregoing arguments - is largely patterned after proved design forms based upon ten years' experience, not only in problems of resistance but also in problems of strength, as well as motion characteristics. Needlessly complicating details, which now and again appear in a single development not - or only partially - utilizing the possibilities of the research, have been left out.

The need for being able to vary the length-beam ratio l_L/b_{st} and the included angle of dead rise ζ, to suit a particular purpose, leads to families of related floats, for which the investigation must be made on such a wide range of selected loads, trims, and speeds that for every suitable position determined in conjunction with an airfoil, the test values can be obtained by interpolation within the curve system, providing that no stages already defined by limiting curves are reached in which the float becomes unsuitable with respect to resistance or spray formation. The best coordination of the float system to the airfoil of the project follows on the basis of the measurements. This method was suggested by Seewald (reference 5) used in the N.A.C.A. tank (reference 6), and further developed by the DVL.

The design of the six models investigated so far:

l_L/b_{st}	6.04	7.50	9.19
Family A: $\zeta = 140^\circ$	Model 1a	8	7
" B: $\zeta = 130^\circ$	" 17	18	19

is shown in figure 14. The beam of the model is b_{st} = 0.3 m. The models of a family are developed from the basic form (smallest l_L/b_{st}), by starting at the step and increasing the spacing of the sections of the forebody and afterbody along the keel tangent in the ratio to the model lengths. Depth of step and angle between forebody and afterbody remain constant for all models. The related models of the two families are congruent in center-line section and plan. The vertical depths of section (measured from base of section) are to one another as the dead rises $\tan \frac{180 - \zeta}{2}$.

The models have vertical sides and straight deck. No attempt was made to give the upper part of the float a special form, since discrepancies in the form of the sides can influence the test data only at the beginning of the take-off and even then, only to a negligible extent. The form of the upper part is left to the constructor.

VI. METHOD OF TOWING

The ranges in which a float system is to be investigated are set off:

1) The speed range is given by the Froude number F = 10, corresponding to an assumed high take-off speed;

2) The load range: The load limit depends upon the length-beam ratio. It lies at around $c_a' = 3$ for slender floats. The program of investigation contemplates an increase of the test points at high loads in the zone of maximum resistance; in contrast, the small loads are investigated only in the upper speed range. As the investigation proceeds, it can be seen in what direction the

scheme must be enlarged, so that all important conditions are included.

3) The range of angle of attack: The minimum resistance of a planing surface falls between 4° and 6°. The float system has the tendency to assume high angles of attack (up to $\alpha \approx 10^\circ$) at maximum resistance, and with increasing speed to drop to small angles as the result of the backward shifting of the resultant water force. To insure a short take-off, it is pulled up before get-away to a highest possible angle. From this it follows that in the region of maximum resistance the angles of from 5° to 11° and - in the succeeding stage up to get-away - the angles of from 3° to 9° must be investigated; steps of 2° each are, in general, sufficient.

Presentation of the Results

Form of flow.- As an example, the test points for DVL model 7 at $\alpha = 7^\circ$ constant are given in figure 15 in the form

$$c_a' = f_{(F)}$$

The points are so well identified in the accompanying legend that the characterization of the development of the flow over the model can be obtained from them.

Resistance and moment.- The results are given in figure 16 in nondimensional form:

$$\epsilon = \frac{W}{A} \quad \text{and} \quad c_{mh} = \frac{M_{h_{st}}}{\gamma\, b_{st}^4}$$

against

$$F = \frac{v}{\sqrt{g\, b_{st}}}$$

with the parameter

$$c_a' = \frac{A}{\gamma\, b_{st}^3}$$

whereby the moment M_{st}, referred to the keel at the step can be computed from the moments obtained in the test. This presentation affords, on the basis of Froude's law of

model similitude, a possibility of comparison with the results from other models: If one imagines that the models to be compared are all enlarged to a unit beam, the speed v for equal Froude number F is the same, and for equal load coefficient c_a', the lift A is likewise the same, so that the glide numbers ϵ and the moment coefficients c_{mh} are directly comparable.

Plotting $\epsilon = f(\alpha)$ separately with F as the parameter for c_a' as the curve constant, figure 17 gives with c_a' as the parameter a curve of α_{opt}, for which the corresponding ϵ is a minimum.

Center of buoyancy and water line at rest.- The initial attitude of the float system for any loads and any position of the center of gravity, is determined from figure 18 where, in nondimensional form, the horizontal distance l_{st} of the center of buoyancy $\odot_D$ from the step and the vertical distance of the water line above the keel at the step t_{st} is given as a function of α with c_a' as the parameter.

Interpolation of the Results

The scope of possible application of the experimental data is increased if freedom exists in the choice of length-beam ratio and angle of dead rise within the range of the families of floats investigated; i.e., if by interpolation of the test data the measurements are equally applicable to designs with intermediate values of l_L/b_{st} and ζ. Figures 19 and 20 show for all six models at $\alpha = 9^\circ$ ϵ and $c_{mh} = f_{(F)}$ and at α_{opt} $\epsilon_{min} = f_{(F)}$ a series of loads corresponding to a normal float system, which is given by $c_a' = c_{a_o}' (1 - 0.01 F^2)$ at $c_{a_o}' = 1.70$, thus including all the models.

The curves of the floats of one family as well as the correlated floats of both families manifest such a similar course while the differences are so small that the application of the results to intermediate values by linear interpolation is justified.

VII. APPLICATION OF THE RESULTS

Choice of Dimensions

With the size of the float approximately determined from design requirements, the beam also is determined. A change in dimensions with regard to take-off resistance is usually possible only within narrow limits. A control is set up according to the diagram (fig. 21).

At three critical speeds: for instance, at maximum resistance, at 0.6 v_{start}, and 0.85 v_{start}, ϵ is plotted from the optimum sheet as $f(c_a')$ (at maximum resistance the envelope curve is taken from the maxima of different load stages and used with a medium Froude number). The hydrodynamic load A^+ and the air drag W must be determined approximately for the particular speed stages. It is then possible from the ϵ values of the above figure to give a rough course of the water resistance and also of the total resistance, as in figure 22, for any beam that may be of interest, from which a suitable beam can finally be definitely determined. The length is checked by repetition for different values of l_L/b_{st}.

Coordination of Wings and Float

The problem is so to choose the angle of setting σ_1 between wing chord and planing bottom that the take-off occurs at minimum resistance. The best setting at the three speed stages named is determined according to figure 23. For v = constant (0.85 v_{start}, for example), we plot against the angle of attack of the wing α.

The aerodynamic lift A and the hydrodynamic lift A^+, in which $A^+ = G - A$:

Then $c_a'^+ = \frac{A^+}{\gamma\, b_{st}^3}$. The corresponding ϵ_{min} and α^+_{opt} for this $c_a'^+$ curve are obtained from the optimum sheet. From this the water resistance $W^+ = \epsilon_{min} A^+$ is determined.

When the air resistance W is determined, we have

the total resistance of $W_{total} = W^+ + W$. If the minimum of this lies, say, at α_1, for which $\alpha^+_{opt} = \alpha^+_2$, then $\sigma_1 = \alpha_1 - \alpha_2^+$.

The degree of freedom to diverge from $\sigma_{1_{opt}}$ for design reasons, depends upon whether the total-resistance curve is flat or reveals a distinct minimum. The best setting in the upper speed range is usually quite constant, but diverges from it more or less at maximum, so that σ_1 must be averaged.

Position of Center of Gravity
Equilibrium of Moments

For the temporary center-of-gravity position assumed in the design, we establish, according to figure 24, for a sufficient number of speed stages the equilibrium of the moments between hydrodynamic and aerodynamic total moment (with the most exact possible consideration of the slipstream effect and ground effect) for take-off with neutral elevator and for maximum positive and negative elevator deflection.

In the speed range between maximum resistance and about $0.85 v_{start}$ the airplane should have the lowest possible total resistance without elevator operation; i.e., should take off with neutral elevator. At maximum resistance itself, "pushing down" is usually necessary, and in the upper speed range, of course, an increasing pull-up. If the calculation does not give this desired behavior for the position of the center of gravity initially assumed, the center of gravity must be shifted relative to the step and the calculation repeated.

On the basis of the curves of the temporary total resistance for take-off with neutral elevator and with maximum positive and negative elevator deflection, a take-off specification can now be set up covering the movement of the elevator for insuring the best take-off.

VIII. COMPARISON OF THE DVL STANDARD FLOAT* WITH THE N.A.C.A. MODEL NO. 35

From the many foreign float designs on which model test data are available, the N.A.C.A. model No. 35 (reference 7) stands out for its good resistance characteristics. Figure 25 gives the result of a comparative test; $\epsilon = f_{(F)}$ is plotted with α as the parameter. Both models have the same length, beam, and dead rise, and were towed with the same load schedule simulating unloading by wings.

The comparison shows that, at maximum resistance, the best resistance of the N.A.C.A. float at $\alpha = 7^\circ$ is 3 percent less, but that at the higher angles at which a float at maximum resistance actually runs, it is considerably worse; that is, by 13 percent at $\alpha = 9^\circ$, and 15 percent at $\alpha = 11^\circ$. In pure planing condition the N.A.C.A. model is considerably inferior at all angles, which can only be ascribed to the unfavorable form given to the pressure area by the pointed step. The resistance curves do not cross until speeds shortly before get-away, where the small, high afterbody surface of the N.A.C.A. model can influence the resistance favorably because of less wetting. While the standard float yet allows a 7° setting and only runs on the afterbody at 9°, the N.A.C.A. float already runs on the afterbody at 7° - a condition which at get-away can only be realized by having large control surface moments available. The get-away speed of the N.A.C.A. float must therefore be set higher than the standard float. The N.A.C.A. float also shows a considerably more unfavorable spray pattern on account of the absence of recurvature at the chine.

IX. FINAL REMARKS

The purpose of the development of a good type of float has been attained, as the above and other comparisons show. The making of the large number of tests that were necessary to make the float generally applicable was therefore worth-while. However, it is not asserted that the float will also show the best characteristics in all dimensions and conditions of load. (Cf. requirements under d), p. 4.) Tests with dynamically similar models capable

*From the family C with $\zeta = 150^\circ$ in course of investigation.

of flying are in progress so as to ascertain these characteristics also for the total range of the standard float, since English experiments (reference 8) have proved the feasibility of such tests and their extension to full size.

As an example of the application of the standard float, figure 26 shows the Ha 139, a four-engine twin-float seaplane built by the Hamburg Airplane Corporation for the Luft Hansa, which is noted for its very short take-off time and pleasing take-off and landing characteristics.

Translation by J. A. Vanier,
National Advisory Committee
for Aeronautics.

REFERENCES

1. Sottorf: Veröffentlichung in Vorbereitung.

2. Mewes, E.: The Impact on Floats or Hulls During Landing as Affected by Bottom Width. T.M. No. 811, N.A.C.A., 1936.

3. Sottorf, W.: Experiments with Planing Surfaces. T.M. No. 661, N.A.C.A., 1932.

   Sottorf, W.: Experiments with Planing Surfaces. T.M. No. 739, N.A.C.A., 1934.

4. Mewes, E.: Die Stosskräfte an Seeflugzeugen bei Starts und Landungen. VLF-Jahrbuch 1935.

5. Seewald, F.: On Floats and Float Tests. T.M. No. 639, N.A.C.A., 1931.

6. Shoemaker, James M., and Parkinson, John B.: A Complete Tank Test of a Model of a Flying-Boat Hull - N.A.C.A. Model No. 11. T.N. No. 464, N.A.C.A., 1933.

7. Shoemaker, James M., and Bell, Joe W.: Complete Tank Tests of Two Flying-Boat Hulls with Pointed Steps - N.A.C.A. Models 22-A and 35. T.N. No. 504, N.A.C.A., 1934.

8. Coombes, L. P., Perring, W. G. A., and Johnston, L.: The Use of Dynamically Similar Models for Determining the Porpoising Characteristics of Seaplanes. R. & M. No. 1718, British A.R.C., 1935.

   Perring, W. G. A., and Hutchinson, J. L.: Full Scale and Model Porpoising Tests of Singapore IIC. R. & M. No. 1712, British A.R.C., 1936.

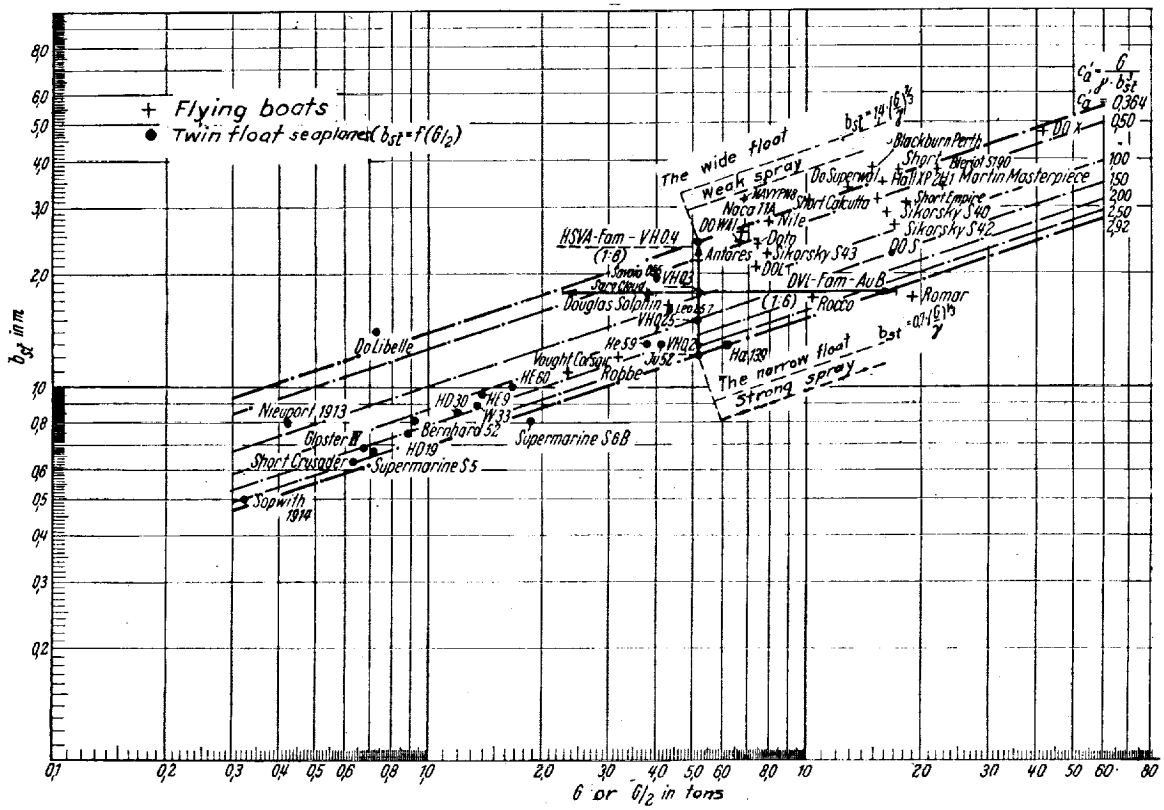

Figure 1.- Beam at step of various airplanes against gross weight.

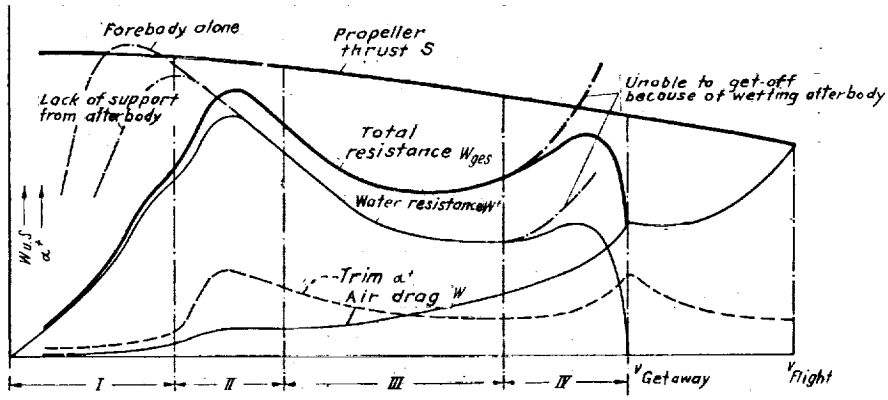

Figure 3.- Take-off diagram.

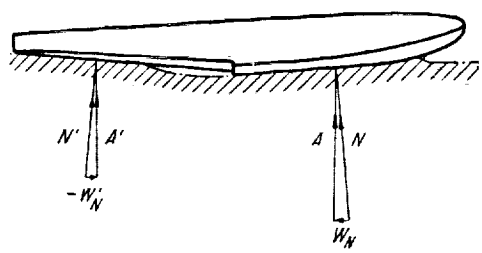

Figure 4.- Flow paths and forces at stage I.

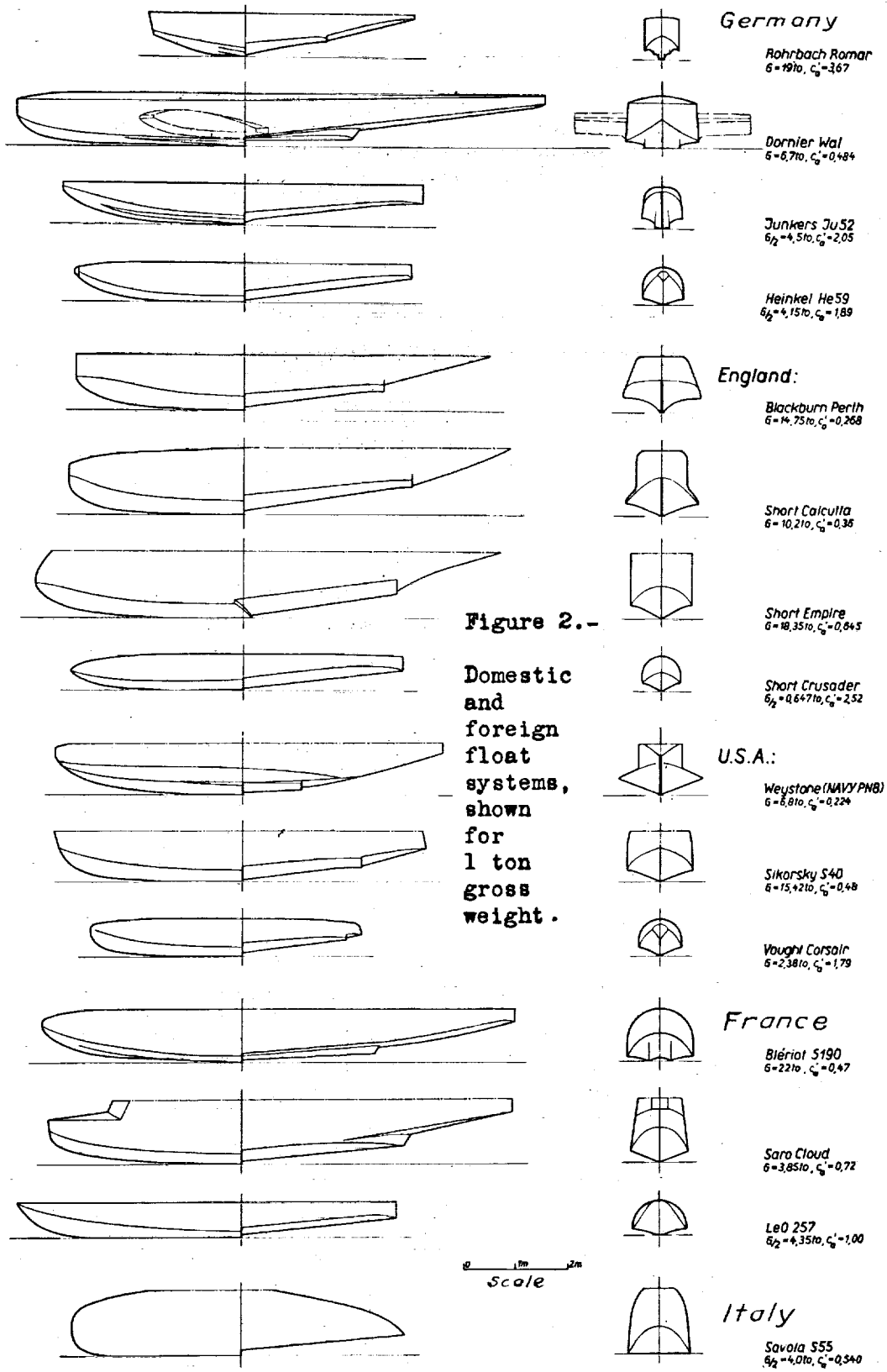

Figure 2.- Domestic and foreign float systems, shown for 1 ton gross weight.

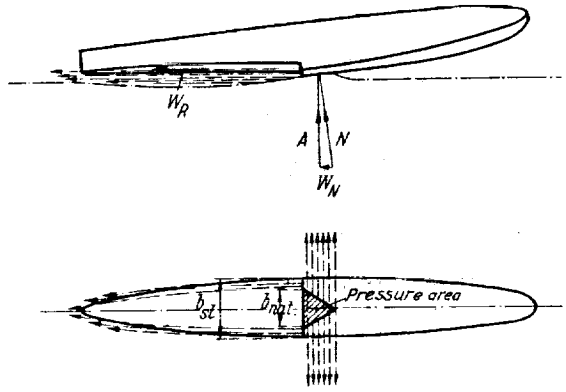

Figure 5.- Flow paths and forces at stage IV.

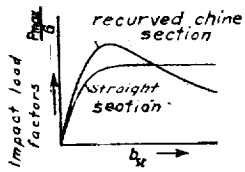

Figure 8.- Impact load factor against beam of float.

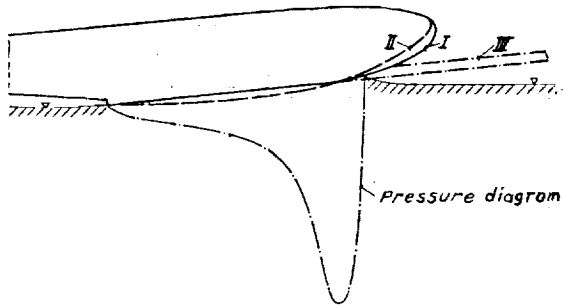

Figure 9.- Diagram showing different curvatures of the forebody.

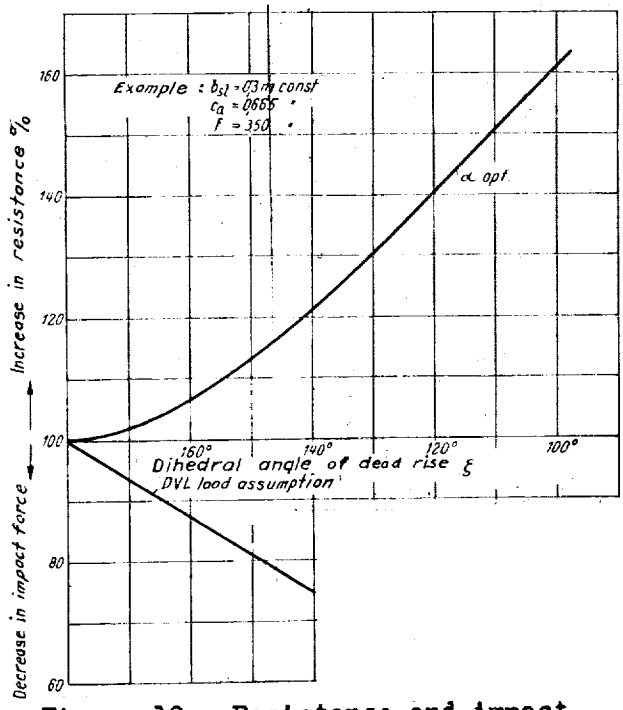

Figure 10.- Resistance and impact force against included angle of dead rise.

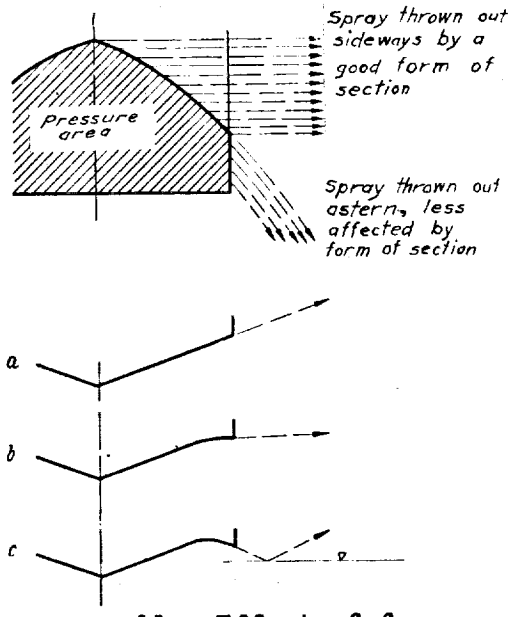

Figure 11.- Effect of form of section on deflection of spray.

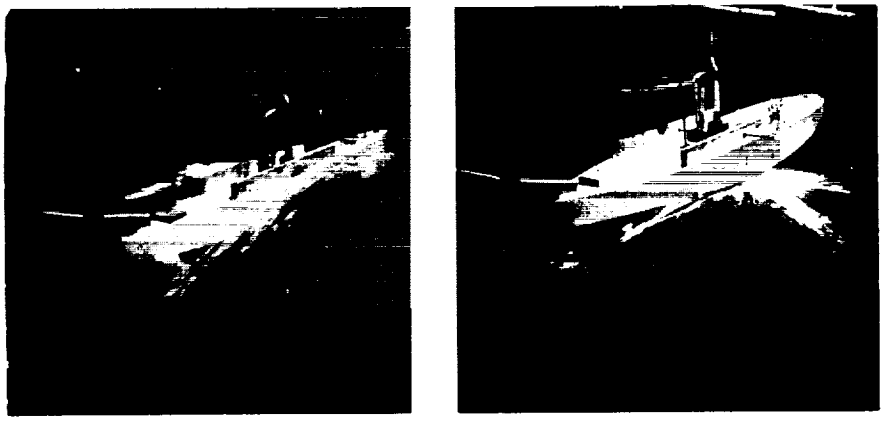

Figures 6,7.- Comparison of spray of model 0.2 VH (b_{st} 0.2m) and 0.4 VH (b_{st} 0.4m) at the same load 18 kg; speed 6 m/s, trim 6 deg.

Figure 12.- Deflection of spray;
left half: form of section according to figure 11c,
right " " " " " " " 11b.

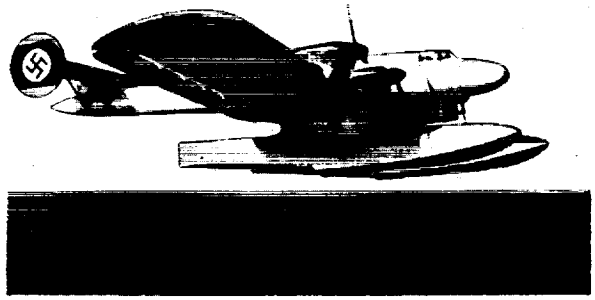

Figure 26.- Ha 139 built by the Hamburg airplane Co. for the Lufthansa.

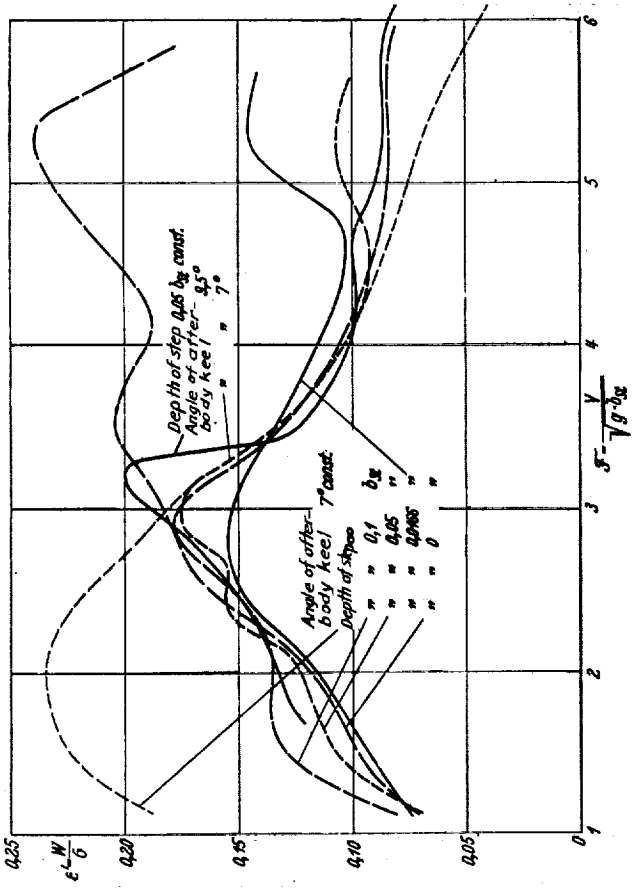

Figure 13.- Effect of depth of step and angle of afterbody on the resistance.

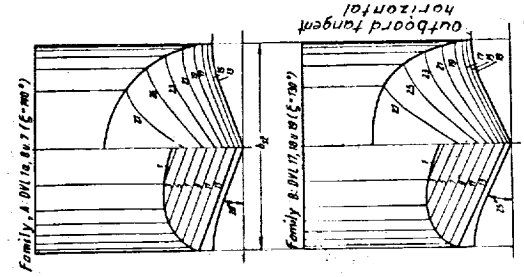

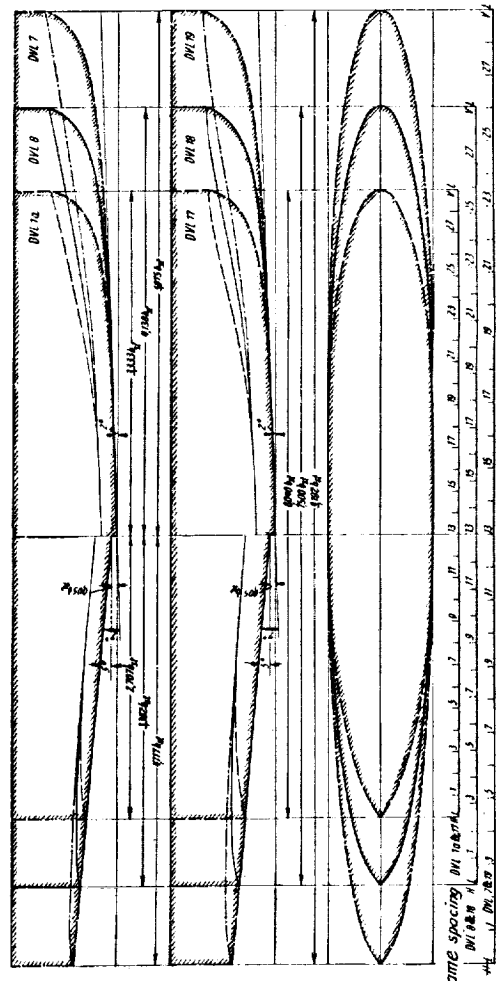

Figure 14.- Plans of DVL standard floats, family A (DVL 1a, 7 and 8) and family B(DVL 17,18,19).

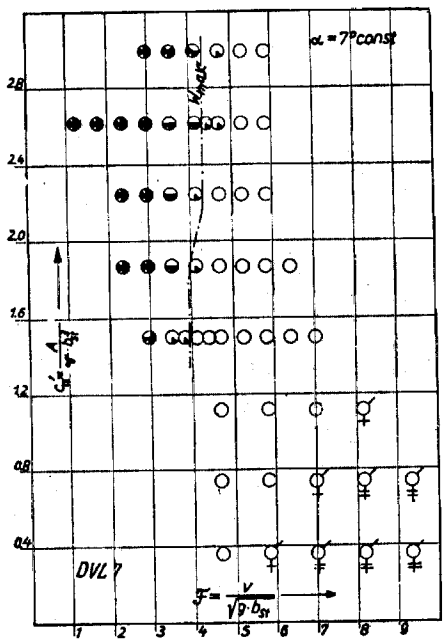

Figure 15.- Test schedule with designation of flow conditions, example for DVL 7, $\alpha = 7$ deg. const.

●	Side and bottom of float wetted- buoyant condition
⊕	As above. Forebody wetted whole length. A blister of water appears at the bow (limit of load).
◐	Left half of circle — sides clear forward only, wet most of length. Condition on sides.
◐	In stages I and II — sides mostly clear, only wet a little, mostly in way of step.
◑	Right half of circle — afterbody bottom hard on water, more than 1/2 length of afterbody
◑	Condition on bottom of afterbody — afterbody bottom on water less hard, 1/4 to 1/2 length of afterbody
◑	In stages I and II — afterbody bottom on water only slightly less than 1/4 of afterbody
○	Stage III — sides of float and afterbody clear of water. Pure planing condition
♀	Afterbody bottom wetted slightly by spray from the step.
♀	Condition on bottom of afterbody — Afterbody bottom wetted strongly by spray from the step
♀	In stage IV — Afterbody bottom wetted very heavily by spray from the step. Unstable condition, measurement of resistance impossible.
♀	Float runs on afterbody only.
♂	In stages III and IV — Natural beam smaller than beam at step.

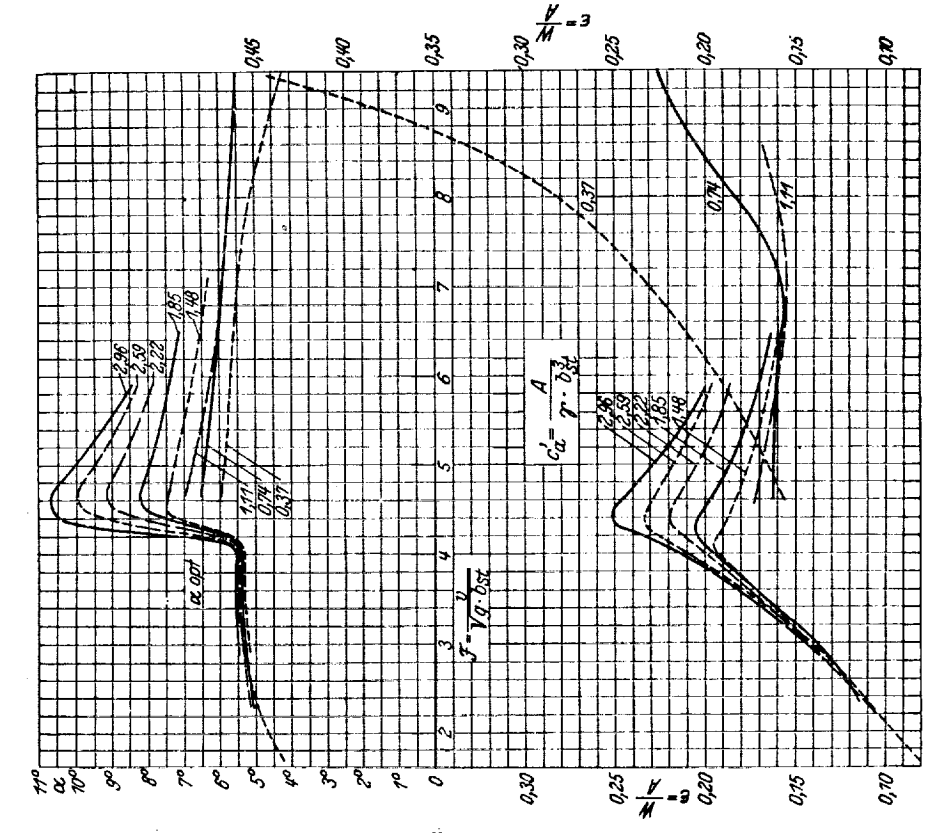

Figure 17.- Optimum resistance and the corresponding trim (best trim).

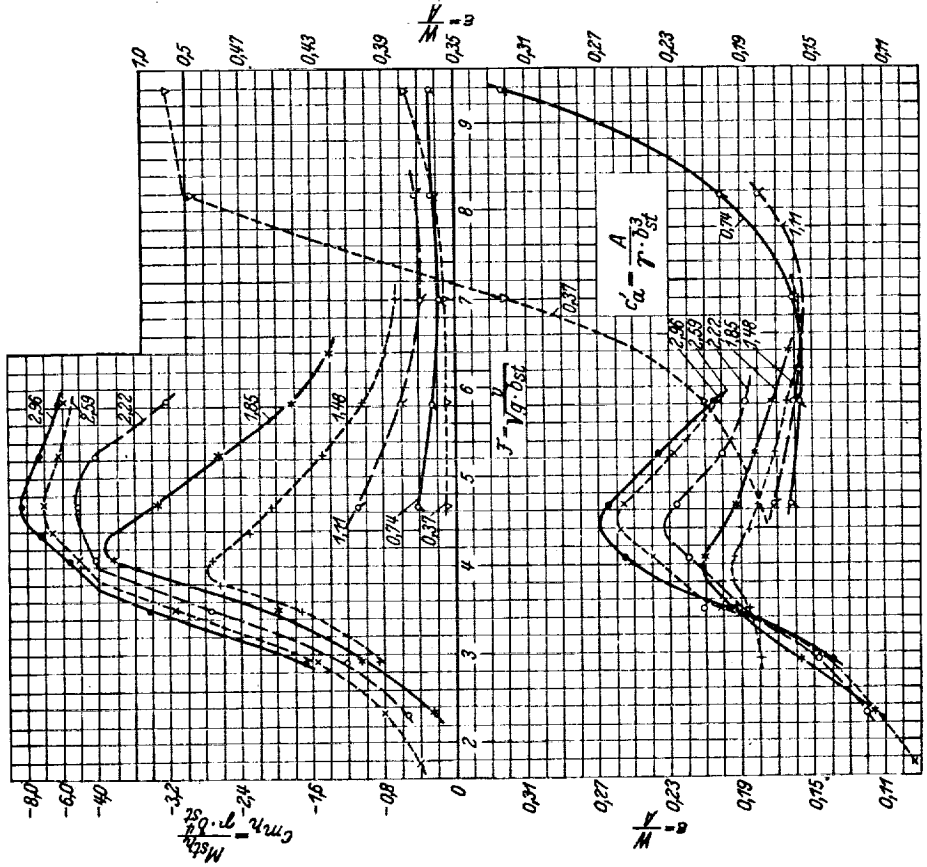

Figure 16.- Resistance and moments; example for DVL 7, $\alpha = 70$ const.

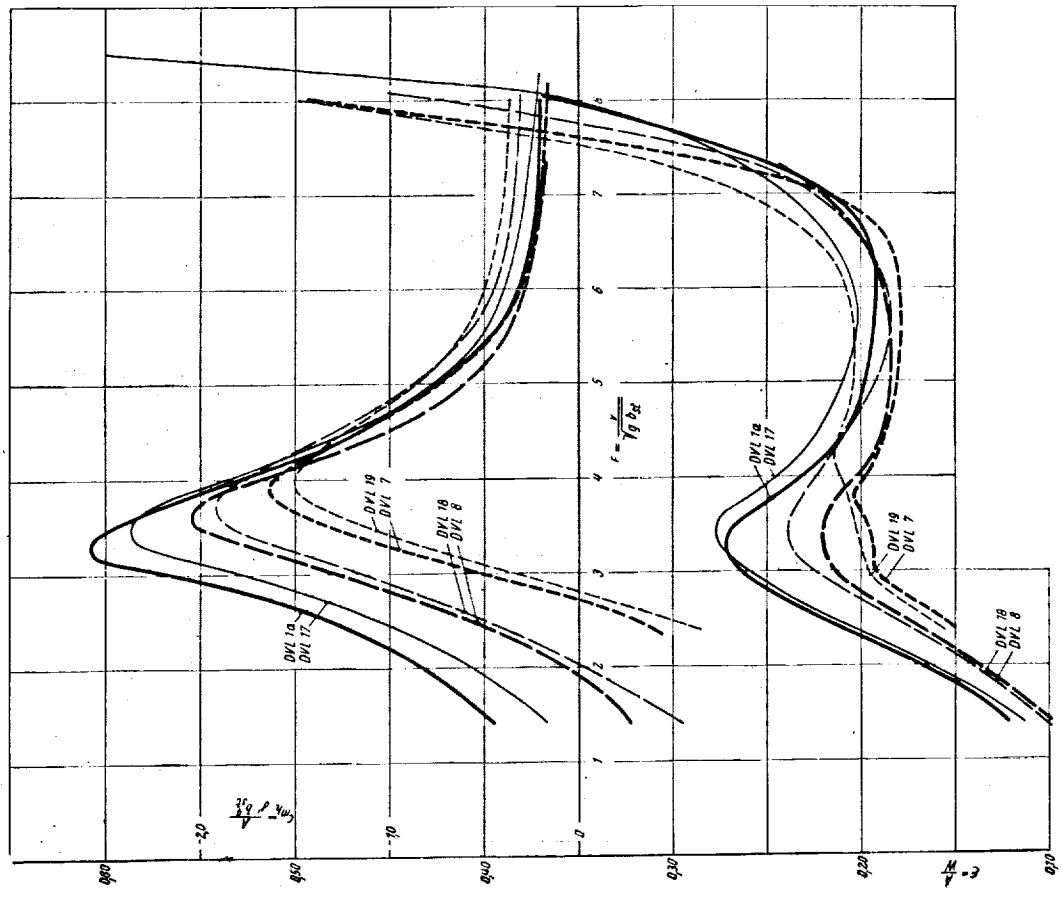

Figure 19.- Resistance and moments for all models at the same load; example $\alpha = 9^0$ const.

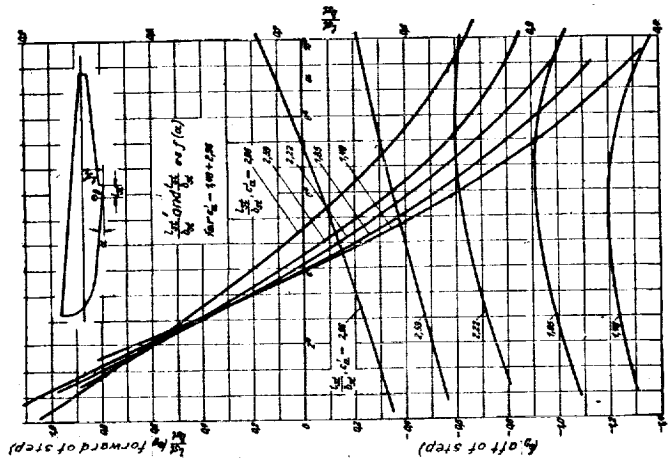

Figure 18.- Position of center of buoyancy ⊙D and water line against load trim. Example for DVL 7 model.

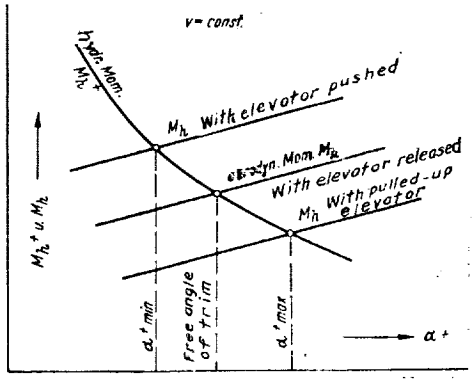

Figure 24.- Equilibrium of moments.

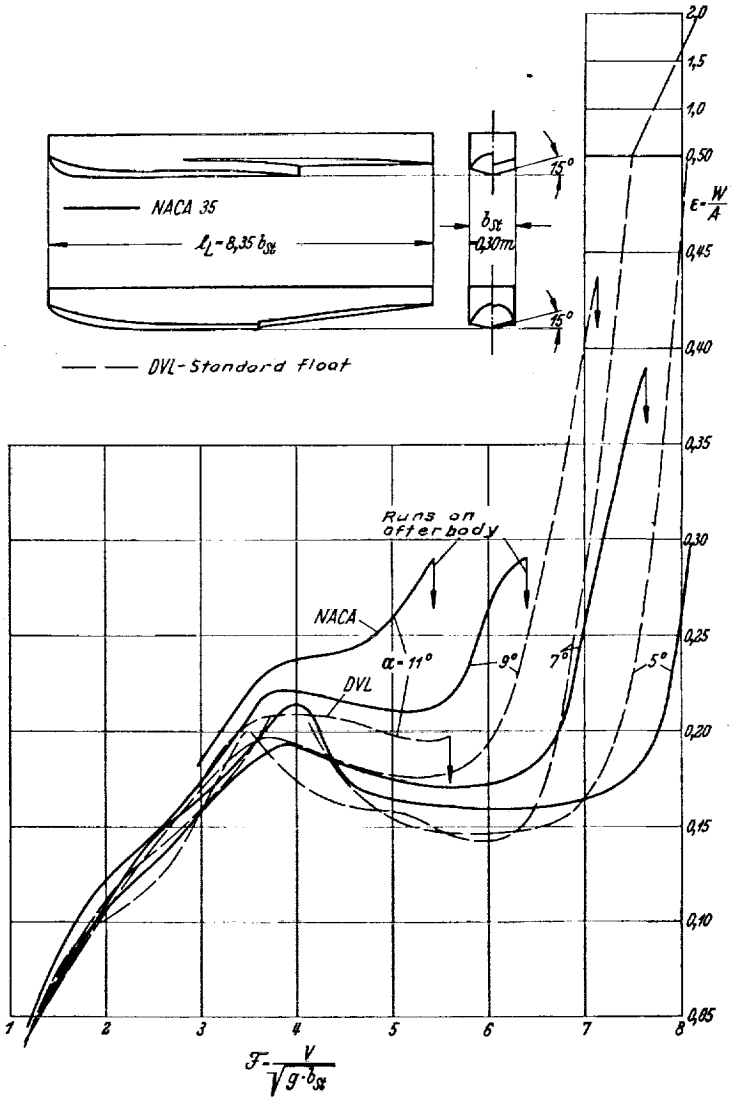

Figure 25.- Comparison of DVL standard floats with the N.A.C.A. model No. 35.